

JSACE 2/29

Influence of Different  
Waste Materials on  
Resistance of Cement  
Mortars against  
Carbonation and  
Chloride Ingress

Received  
2021/05/30

Accepted after  
revision  
2021/10/05

# Influence of Different Waste Materials on Resistance of Cement Mortars against Carbonation and Chloride Ingress

**Nikolaos Chousidis**

Department of Materials Science and Engineering, School of Chemical Engineering, National Technical University of Athens. Athens, Greece

Department of Structural Engineering, School of Civil Engineering, National Technical University of Athens. Athens, Greece

**George Batis**

Department of Materials Science and Engineering, School of Chemical Engineering, National Technical University of Athens. Athens, Greece

\*Corresponding author: [nickhous@central.ntua.gr](mailto:nickhous@central.ntua.gr)

 <http://dx.doi.org/10.5755/j01.sace.29.2.29208>

This work is an extensive experimental study on the corrosion behavior of reinforced cementitious mortars containing industrial byproducts and waste materials. In particular, calcareous (C-class) fly ashes, iron mill scale and Electrolytic Manganese Dioxide (E.M.D.) waste were used as additives in mortars production. The abovementioned materials were used without any prior treatment or management and replaced the cement in concrete mixing by 10% wt. of cement weight. For the experimental set-up, reinforced mortars were prepared and exposed to coastal area for 12 months, while some of them were remained in a salt spray cabin for 60 days. The corrosion monitoring was performed by electrochemical and mass loss measurements, while chloride content, porosity, carbonation and mineralogy of mortars were also estimated. The results indicate, that there is a development in durability and chloride penetration resistance of composites comparing with the conventional mortars at late ages. At the same time, it was also observed that their chemical composition and fineness, control the diffusion of CO<sub>2</sub> into the pore system and lead to increased carbonation of composite mortars. The challenge of this work is the production of eco-friendly composites with high chloride and carbon dioxide penetration resistance.

**Keywords:** waste materials management; reinforced mortars; carbonation; chloride-induced corrosion; electrochemical measurements.

## Introduction



The corrosion of reinforcing steel in concrete is a major problem for the engineers throughout the world; at the same time, the presence of cracks in carbonated concrete is unavoidable leading to corrosion of steel reinforcing bars. There are several methods for preventing or delaying the penetration of chlorides and the corrosion of reinforcement steel in concrete, such as organic inhibitors, coatings, electrochemical methods (cathodic protection, chloride extraction, re-alkalization etc.) (Za-feiropoulou et al., 2013), (Vyrides et al., 2013). These methods have some drawbacks, such as the high maintenance cost and/or toxicity. A relatively inexpensive way for improving the resistance of reinforced concrete against chloride penetration is the utilization of industrial by-products or waste materials as substitutes of cement and/or aggregates during concreting (Chousidis et al., 2015a).

In construction industry usually used industrial by products as supplementary materials (SCMs) such as fly ash, blast furnace slag or silica fume, (Shaikh and Dobson, 2019), (Yodsudjai et al., 2020) (Joshaghani et al., 2018), (Wang et al., 2014); these additives can be utilized in high amounts (up to 65% wt.) replacing the cement content in concrete. Previous studies (Chousidis et al., 2020), (Chousidis et al., 2018) have been conducted to identify the benefits afforded by adding waste materials to Portland cement in terms of the performance of the resulting concrete when exposed to different aggressive media such as sulphates, chlorides and so on. In these studies, the experimental results show that the waste materials provide anticorrosion protection on the reinforcement steel against chlorides; at the same time, the addition of fine-grained or pozzolanic materials leads to enhancement of the strength of the reinforced concrete and reducing its porosity (Shaikh et al., 2018), (Shaikh and Dobson, 2019), (Menadi et al., 2009), (Krishnamoorthi and Kumar, 2013). In fact, fly ash additive reacts with the cement compounds (pozzolanic activity) affecting on the Calcium Silicate Hydrate (C-S-H) formation which is the main hydration product of Portland cement and is primarily responsible for its strength development (Qian et al., 2001), (Chousidis et al., 2015b). Generally, the abovementioned industrial by-product comes in the form of spherical particles improving the workability of blended cements, while its reactivity is a function of its chemical/mineralogical composition, particle size, and amorphous content (Mehta and Gjrv, 1982), (Zhao et al., 2015), (Bhagath Singh and Subramaniam, 2017). However, the corrosion resistance of reinforced concrete depends on the protective film surrounding the surface of steel or the nature of the hydration products of hardened cement paste (Shi and Stegemann, 2000).

On the other hand, ultrafine materials due to their small particle size may increase the chemical reactivity with the cement compounds to create carbonate salts into the pores (Chousidis et al., 2016b). In the literature (Choudhary et al., 2021), (Seleem et al., 2020), it has been also investigated the beneficial effect of ultrafine materials on the pitting corrosion of steel rebars exposed to chloride ions. The experimental results showed that the time to the initiation of reinforcement corrosion in specimens with 8% wt. and 10% wt. ultrafine materials was 230 days and 130 days, respectively; the aforementioned researcher also proved the reduction of chloride diffusion coefficient with depth in concretes with up to 10% wt. additive. In this study, steel mill scale generated during processing of iron in steel mills, was used as cement substitute. During the manufacturing of the structural steel in the mill, iron oxides (wstite, hematite etc.) are formed on the surface of the metal during the continuous casting, reheating and hot rolling operations; the steel mill scale is removed by water sprays. The aforementioned material has a small particle size and added in small amounts ( $\leq 10\%$  wt.) during concrete production; it reacts with C - H to form carbonate salts such as ankerite  $[\text{Ca}(\text{Fe},\text{Mg},\text{Mn})(\text{CO}_3)_2]$  and siderite  $[\text{FeCO}_3]$ . Due to its high specific surface and small grain, the addition of mill scale leads to decreased porosity values and corrosion rates, as expected.

It is worth noting that the influence of Electrolytic Manganese Dioxide (E.M.D.) waste and iron mill scale (SLA) in the performance of reinforced mortars has not been studied extensively to-date; up to now, these materials are currently being disposed to landfill sites without any prior treatment or management. Iron mill scale often consists of hydrocarbons ( $\geq 1\%$  by weight) on its surface such as oil and grease which are deleterious to the environment; for this reason, the iron mill scale usually used in the production of Portland cement clinker ( $T > 1400\text{ }^\circ\text{C}$ ). On the other hand, E.M.D. waste includes significant amounts of heavy metals such as Pb, As Ni, Zn and Cd, the values of which generally exceed the permissible limits set by various international organizations (US EPA, EU, WHO) (Chousidis et al., 2018). Regarding the FAs used as admixtures in the present study, they are not classified in accordance with International Standards for the production of cementitious composite materials due to their chemical composition, mineralogy and/or physical characteristics (high sulphate and carbon contents, low glass phase and so on); however, due to their fineness and/or pozzolanicity may be used as SCMs in the production of cement-based materials.

## Preparation and Corrosion Monitoring of Reinforced Mortar Mixes

The aim of this work is the utilization of unclassified additives for the production high performance reinforced mortars against chlorides and carbonation; these additives such as mill scale and FAs are usually used in construction; however, these pozzolans consist of high free CaO and SO<sub>3</sub> amounts, while the iron mill scale is usually exploited for the clinker production or in high-density concretes. Last but not least, E.M.D. waste consists of sulfate compounds such as gypsum and jarosite in its composition.

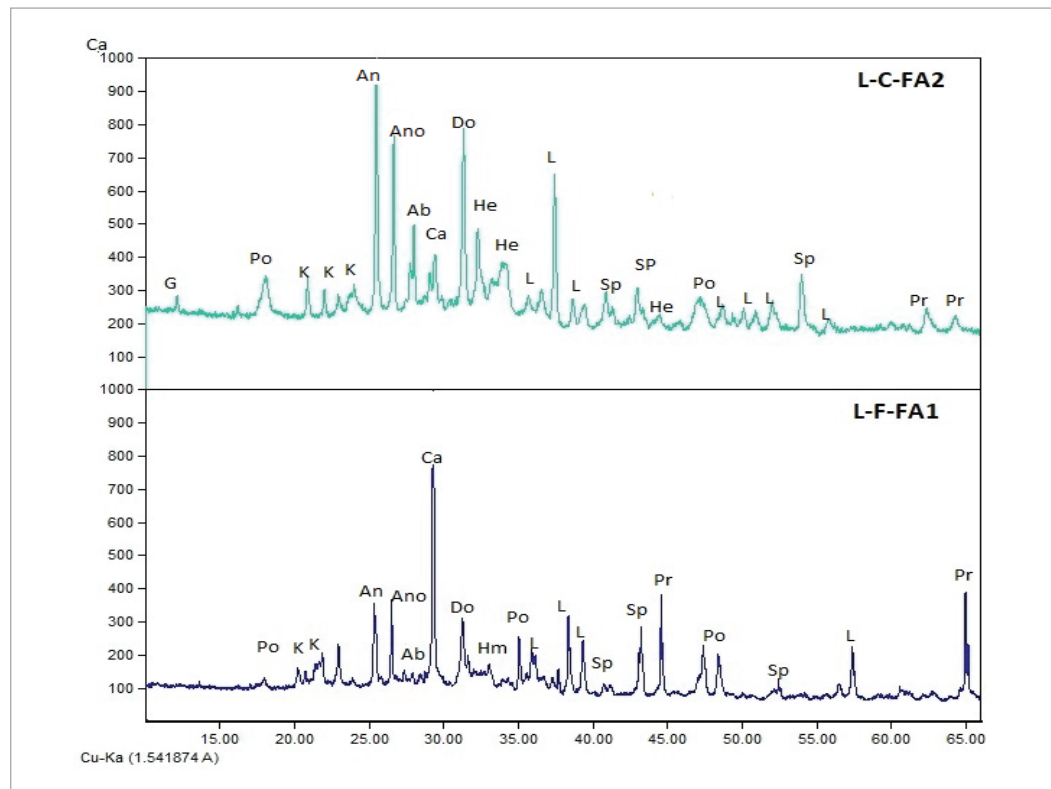
### Raw materials and sample preparation

The test samples were prepared using CEM I 42.5 N, water from the supply network and fine (0 – 4 mm) aggregates. In the current research, four (4) waste materials and industrial products were used as cement replacements in mortars production; (i) two (2) lignite fly ashes (FAs) enriched in SiO<sub>2</sub> (code: L-C-FA2) and SO<sub>3</sub> (code: L-F-FA1), (ii) iron mill scale (code: SLA) generated during the hot-rolling process and (iii) a waste material generated by Electrolytic Manganese Dioxide (code: E.M.D.). The latter additive is enriched in ferrous sulfate, iron oxides, jarosite and goethite; E.M.D. waste also contains trace elements and impurities such as Cu, Ni, Co, Zn, and Fe etc. (Panda et al., 2009). The precise replacement level of cement with waste materials was 10% wt. by weight of cement. Iron mill scale, E.M.D. waste and FAs were obtained from Halyvourgiki Hellenic Steel Industry S.A., TOSOH HELLAS A.I.C. and TITAN CEMENT A.E., respectively; their physical properties and the mineralogical characteristics have been analyzed in previous experimental works (Chousidis et al., 2015b), (Chousidis et al., 2015a), (Chousidis et al., 2016b), (Chousidis et al., 2018), (Chousidis et al., 2016a). Fig. 1 and 2 illustrate the mineralogical composition of FAs and iron mill scale, respectively, while the physic-mechanical properties and the compositions of raw materials are shown in Tables 1, 2 and 3. As can be seen in Table 3, the two fly ashes used in the study consist of significant amounts of SO<sub>3</sub> and CaO; the aforementioned chemical compounds present in the form of anhydrite and lime, respectively (Fig. 1). It is worth noting that the elevated content of free CaO causes soundness problems in

Fig. 1

XRD patterns of two fly ash samples used in the study.

(Po: portlandite, K: kaolinite, An: anhydrite, Ano: anorthite, Ab: albite, G: Gypsum, Ca: calcite, Do: dolomite, Hm: hematite, L: lime (CaO<sub>total</sub>), Sp: spinel, Pr: periclase)



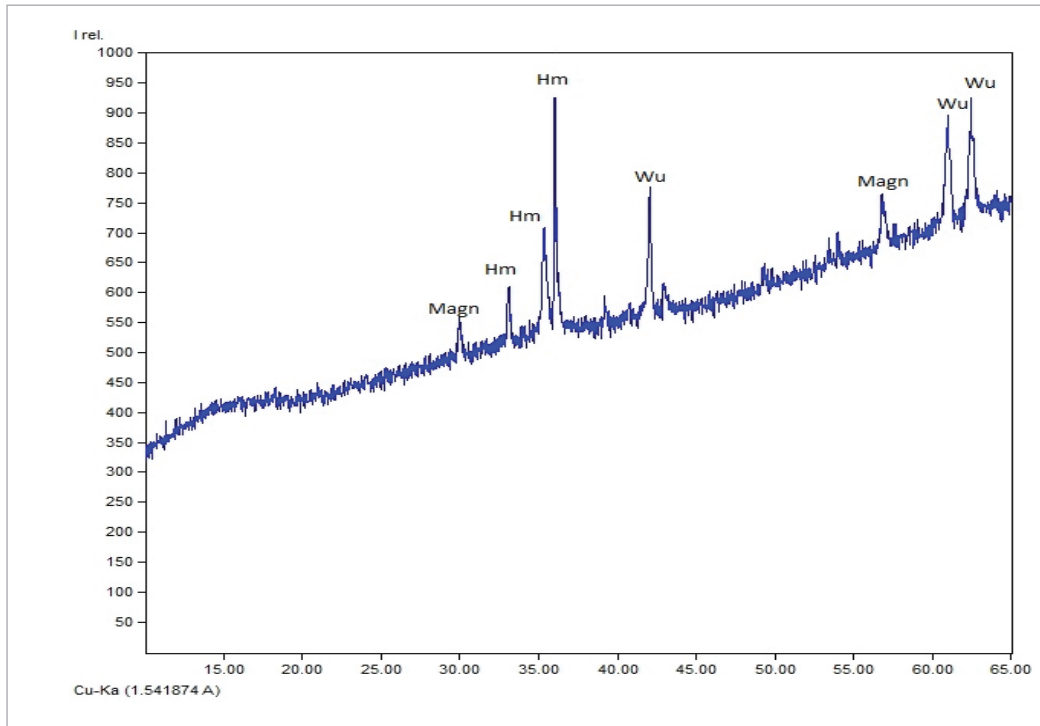


Fig. 2

Diffraction pattern of iron mill used in the study (Chousidis et al., 2020). (Magn: magnetite, Wu: wüstite, Hm: hematite)

concrete as well as significant temperature increase, (Schlorholtz, 1998). At the same time, high amounts in sulfate ions cause concrete expansion (Zhang et al., 2013), (Ramezani-pour et al., 2020), (Chen et al., 2020). At the same time, the composition of fly ash mainly includes oxides  $\text{SiO}_2$ ,  $\text{Al}_2\text{O}_3$  and  $\text{Fe}_2\text{O}_3$ . These oxides are usually present in the form of amorphous analumino-silicate spheres that react with the cement (pozzolanic reaction).

	Specific gravity	Blaine fineness
<b>Cement</b>	3.15	400 m <sup>2</sup> /kg
<b>Rhenish FA (L-F-FA1)</b>	2.63	380 m <sup>2</sup> /kg
<b>Ptolemais FA (L-C-FA2)</b>	2.56	560 m <sup>2</sup> /kg
<b>Iron mill scale (SLA)</b>	5.41	630 m <sup>2</sup> /kg
<b>E.M.D. waste</b>	4.23	475 m <sup>2</sup> /kg

Table 1

Physical properties of raw materials

	Cement	Iron mill scale	E.M.D. waste
<b>C<sub>3</sub>S + C<sub>2</sub>S</b>	82.41%	<b>Hematite</b> 55.00%	<b>Jarosite</b> 9.20%
<b>C<sub>3</sub>A</b>	6.63%	<b>Magnetite</b> 17.50%	<b>Iron oxides</b> 19.50%
<b>C<sub>4</sub>AF</b>	10.96%	<b>Wüstite</b> 27.50%	<b>Ferrous sulfates</b> 62.80%
			<b>Goethite</b> 8.50%

Table 2

Physical properties of raw materials

Chemical composition (ASTM C-311)											
	SiO <sub>2total</sub>	SiO <sub>2glass</sub>	Al <sub>2</sub> O <sub>3</sub>	Fe <sub>2</sub> O <sub>3</sub>	CaO <sub>total</sub>	CaO <sub>free</sub>	MgO	K <sub>2</sub> O+Na <sub>2</sub> O	SO <sub>3</sub>	Cl <sup>-</sup>	LOI
<b>Cement</b>	19.50	-	4.80	3.60	61.50	-	3.40	0.89	2.60	0.01	3.70
<b>L-F-FA1</b>	14.55	6.24	13.44	6.31	49.80	12.50	3.90	0.99	7.56	-	3.45
<b>L-C-FA2</b>	25.53	11.25	16.80	6.61	40.70	11.50	3.24	1.74	3.38	-	2.00

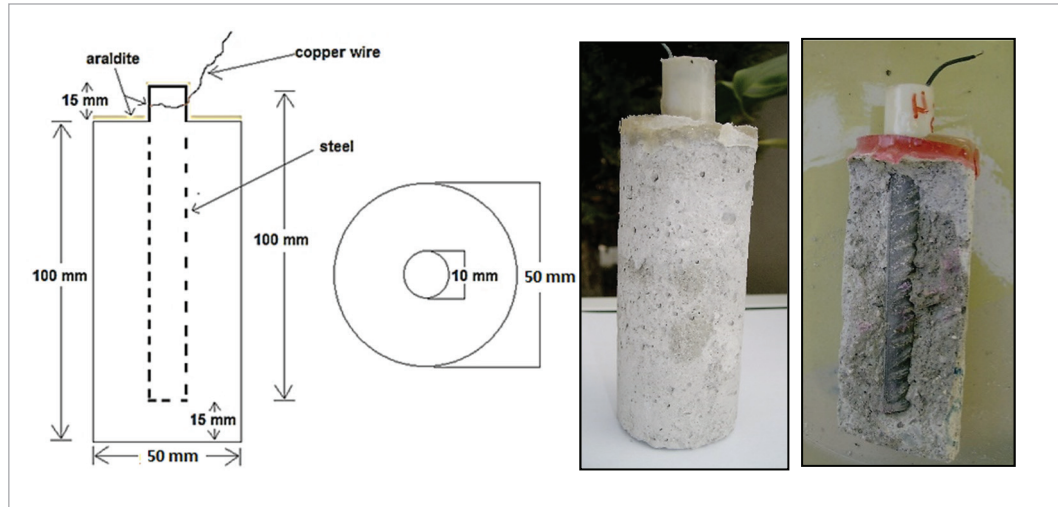
Table 3

Chemical composition of fly ashes and cement used in this study

Weldable reinforcing steel (Tempcore B500C) with diameter  $\varnothing 10$  mm and length  $L=100$  mm was also used and placed axially in the mortars; the steel rebars prior to use were cleaned with water, deionized water and acetone for removing the impurities and oxides from their surface. The space between the bottom surface of each specimen and the steel bar was 15 mm (Fig. 3), whilst the top surface was sealed with a suitable epoxy resin (Araldite AY103-1/HY991).

**Fig. 3**

Schematic representation (left) and photos (right) of cement mortars prepared in the lab



For each group, 100 mm height and 50 mm diameter cylinders were cast and demolded after 24 h (Fig. 3). For the casting, oiled polymer molds were used, while the compaction was performed using a vibrating table for 15 sec. All specimens were demolded 24 hours after casting and, subsequently, they cured in a water tank (25 °C) for 7 days; afterwards, most of the test specimens were exposed to coastal environment, while some of them were also placed in a salt spray cabin with high concentration of chloride ions (5% wt. NaCl and  $T=35^{\circ}\text{C}$ ). In general, five (5) groups of mixtures were produced: i) **L-C-FA2** with 10% wt. fly ash originated from Ptolemais area in Greece, ii) **L-F-FA1** with 10% wt. fly ash originated from Rhenish area in Germany, iii) **SLA** with 10% wt. iron mill scale, iv) **E.M.D.** with 10% wt. Electrolytic Manganese Dioxide waste material and v) **control** mortars without any additive for comparing with the other mixtures. For each batch, thirty (30) reinforced cylinders were prepared and the proportions of raw materials are presented in Table 4. The experimental work was carried out at the laboratories of the National Technical University of Athens (Materials Science & Engineering and Physical-Chemistry labs) which are fully equipped for the purposes of the study.

**Table 4**

Proportions of raw materials for mortars preparation

Constituent	Mass of raw materials (g)					
	Control	E.M.D.	L-F-FA1	SLA	L-C-FA2	
<b>Cement</b>	1980	1782	1782	1782	1782	
<b>Sand</b>	5940	5940	5940	5940	5940	
<b>Water</b>	1287	1544	1426	1346	1465	
<b>Additive</b>	-	198	198	198	198	
<b>Water / cement</b>	<b>Water / (cement + additive)</b>					
<b>Control</b>	<b>E.M.D.</b>	<b>L-F-FA1</b>	<b>SLA</b>	<b>L-C-FA2</b>	<b>Cement/Sand</b>	<b>Additive/Cement</b>
0.65	0.78	0.72	0.68	0.74	1/3	1/10

## Methods and techniques

The experimental set-up includes the preparation of cylindrical reinforced mortars specimens (i.e.  $H=100$  mm and  $\varnothing 50$  mm), the corrosion monitoring mass loss and corrosion rate (CR) measurements of the reinforcement steel, while phenolphthalein tests carried out to evaluate the carbonation of the mortars (Table 5). Last but not least, the chloride content into the mortars was also calculated using the  $\text{AgNO}_3$  titration method. The mortars were placed in Aspropyrgos area (industrial and coastal) where the combined effect of  $\text{NaCl} - \text{CO}_2$  prevails. Table 3 summarizes the experimental setup and procedures performed in the present study.

Test samples	Property	Method	Age (month)	Exposure conditions
Mortars	Porosity ( $\rho$ )	MIP	6 <sup>th</sup> & 12 <sup>th</sup>	Coastal $T_{\text{aver}}=22\pm 2^\circ\text{C}$ , $\text{RH}=65\pm 2\%$ $C_{\text{NaCl}}=3.5\%$ wt.
	Current ( $I_{\text{corr}}$ )	LPR	3 <sup>rd</sup> , 6 <sup>th</sup> , 9 <sup>th</sup> , 12 <sup>th</sup>	
	Carbonation	RILEM CPC-18		
	Chloride content	$\text{AgNO}_3$ titration		
Steel rebars	Mass loss	Gravimetric	1 <sup>st</sup> & 2 <sup>nd</sup>	Salt spray cabin $T=35\pm 2^\circ\text{C}$ , $\text{RH}=99\pm 1\%$
	Corrosion Rate (CR)	Faraday's law		

**Table 5**

Experimental setup and procedure for the corrosion monitoring of steel reinforcement

## Corrosion monitoring

To evaluate the corrosion current density ( $I_{\text{corr}}$ ) of steel bars embedded in mortars, electrochemical measurements were conducted. Linear polarization technique (LPR) is a direct current (DC) technique, first introduced by Stern and Geary in 1957. In this study  $I_{\text{corr}}$  was measured on specimens exposed to coastal environment. Linear Polarization resistance tests (LPR) were performed using a Potentiostat (Model 263A) supplied from EG&G Princeton Applied Research and an associated software package to analyze the obtained data. A saturated calomel electrode (SCE) was used as the reference electrode, a carbon bar was the counter electrode while the steel rebar was represented the working electrode. For the polarization resistance tests, the potential was scanned from  $-15\text{mV}$  to  $+15\text{mV}$  (vs  $E_{\text{oc}}$ ) at  $0.2\text{mV/s}$  scanning rate. The corrosion current density can be calculated by the following Equations:

$$I_{\text{corr}} = \frac{\beta_{\alpha} \times \beta_{\beta}}{R_p [2.3 \times (\beta_{\alpha} + \beta_{\beta})]} \quad (1)$$

$$I_{\text{corr}} = \frac{i}{A_{Fe}} \quad (2)$$

Where,  $I_{\text{corr}}$  is the corrosion current density ( $\mu\text{A}/\text{cm}^2$ ),  $R_p$  is the polarization resistance ( $\text{k}\Omega \text{cm}^2$ ),  $i$  is the current ( $\mu\text{A}$ ),  $A_{Fe}$  is the steel rebar area ( $\text{cm}^2$ ) and  $\beta_{\alpha}$  and  $\beta_{\beta}$  are the anodic and cathodic Tafel constants ( $\text{mV}/\text{decade}$ ), respectively.

## Carbonation depth

In this research the carbonation depth was estimated by the phenolphthalein spray test (DE LA RILEM, 1988); for the phenolphthalein solution preparation, 1.0% wt. phenolphthalein was dissolved in 70% wt. ethylic alcohol and 30% wt. distilled water and sprayed to a fresh fractured surface of the samples. The carbonated area was measured using a digital caliper. The depth of carbonation on each sample was measured three times, and the average value was obtained. The abovementioned procedure was performed for the composite blends and the control mixture. The specimens were placed in coastal environment (Table 3) for a total period of 12 months and the measurements were conducted each 3 months.

The carbonation rate was determined according to the Eq. 3, where  $D$  is the average carbonation depth (mm),  $K$  is the carbonation coefficient (mm/year<sup>1/2</sup>) and  $t$  is the time in which the samples were exposed to the CO<sub>2</sub> (year).

$$D = K\sqrt{t} \quad (3)$$

#### Mass loss and corrosion rate of steel rebars

For the mass loss measurements of the steel reinforcement, the mortars were crushed out, their rebars were cleaned from the rust and then weighted according to ISO/DIS 8407 (International Standard Organisation, 2009); for cleaning, the bars were initially washed with water from the supplied network and then immersed for 15 min in a strong HCl solution (10M) with organic corrosion inhibitor (0.35% wt.). The mass loss measurements were performed at 3, 6, 9 and 12 months in coastal environment, while the corrosion rate was calculated at 1 and 2 months of exposure in accelerated corrosion (salt spray chamber). The corrosion rate (CR) of reinforcement steel was estimated using the following equation:

$$CR (\mu\text{m}/\text{year}) = 8.77 \times 10^7 \frac{W}{At\rho} \quad (4)$$

Where,  $W$  is the mass loss (g),  $A$  is the rebar's surface (cm<sup>2</sup>),  $t$  is the time of exposure (h) and  $\rho$  is the density of steel (7.8 g/cm<sup>3</sup>).

#### Mercury Intrusion Porosimetry (MIP)

The MIP tests were performed on cement mortars (1cm<sup>3</sup>) exposed to coastal environment at 6 and 12 months using a Carlo Erba 2000 Mercury porosimeter. This porosimeter also includes a macropore unit, whilst its pressure ranges from 0 to 200 MPa. The contact angle and the mercury surface tension considered were 130° and 0.485 N/m, respectively. The pressures were converted to equivalent pore diameter using the Washburn equation (Washburn, 1921), as expressed in Eq. 5, where  $d$  is the pore diameter (μm),  $\gamma$  is the surface tension (mN/m),  $\theta$  is the contact angle between mercury and the pore wall, and  $P$  is the net pressure across the mercury meniscus at the time of the cumulative intrusion measurement (MPa). The porosity of mortars was estimated using Eq. 6.

$$d = \frac{-4\gamma\cos\theta}{P} \quad (5)$$

$$p = \frac{V_p}{V_d} \times 100 \quad (6)$$

Where,  $p$  is the porosity of the sample,  $V_p$  is the Hg volume and  $V_b$  the apparent volume of the sample.

#### Evaluation of chloride content in mortars

The chloride content in mortars exposed to coastal environment was estimated using the method described by Karl Friedrich Mohr in 1856; this method determines the chloride ion concentration of a solution by titration with silver nitrate (1 N) (Eq. 9). For the experimental procedure, 5.0 g of oven-dried mortar (1 cm depth from its surface) was placed in a flask with 50 mL of HNO<sub>3</sub> (1 M) and 200 mL of distilled water for 24 h; 10 mL of the filtrated solution was inserted into a conical flask with 90 mL of distilled water, whilst 1 mL of potassium chromate indicator (K<sub>2</sub>CrO<sub>4</sub>) was then added (1 g of K<sub>2</sub>CrO<sub>4</sub> in 20 mL distilled water). The endpoint of the titration was observed with the existence of a red-brown residue (Ag<sub>2</sub>CrO<sub>4</sub>) at the bottom of the flask (Eq. 8), which means that the Cl<sup>-</sup> ions have reacted with the Ag<sup>+</sup> ions. It is necessary to mention that the titration can be achieved only in neutral solutions (pH=6.5 – 7.0); for this reason, 2 – 3 ml of sodium hydroxide solution

(0.1 M) was slowly added before the chromate indicator addition, while the solution's alkalinity was simultaneously recording. The concentration of chlorides in the cementitious mortars was calculated using Eq. 9.



$$\text{Chlorides concentration (mg/l)} = \frac{V_1 C_1 M}{V} \times 1000 \quad (9)$$

Where,  $V_1$  is the volume of silver nitrate used for the titration,  $C_1$  is the concentration of silver nitrate (1 N),  $M$  is the atomic mass of chlorine (35.453 u) and  $V$  is the total volume of solution (100 ml).

To estimate the depth of carbonation in reinforced mortars (Fig. 4), the samples were placed for twelve (12) months in coastal and industrial area. It should be pointed out that the mortars were constantly protected by the rain, to eliminate the  $\text{Ca}(\text{OH})_2$  leaching. In general, three (3) carbonation depths were taken for each sample after breaking and spraying with phenolphthalein solution (Fig. 4) and the average values were obtained. The results of carbonation depth are presented in Table 6, while Fig. 5 depicts the carbonation rate ( $\text{mm}/\text{yr}^{1/2}$ ) calculated by Eq. 3.



## Results and Discussion

Fig. 4

Carbonation of mortars with and without additives at 12 months of exposure in coastal environment: from Left to right: Control, E.M.D., L-F-FA1, SLA & L-C-FA2

From the experimental results, it was found that the carbonation increases with the addition of FAs and SLA up to 6 months of exposure in coastal conditions (Table 6); the increase in carbonation depth in these mixes may be due to their high porosity compared to OPC mortar; this is attributed to the higher water contents in com-

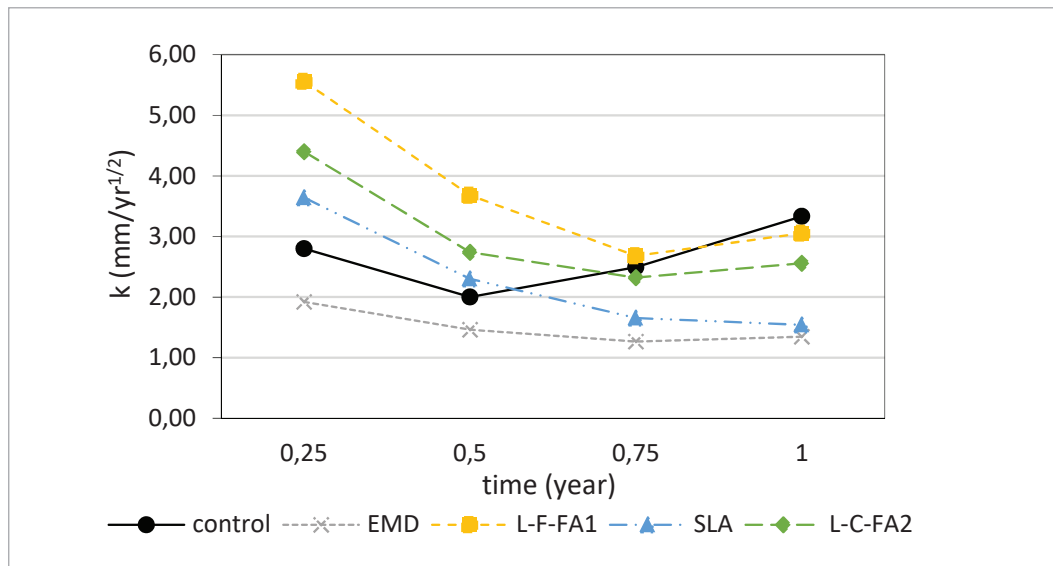
time (months)	Control	E.M.D.	L-F-FA1	SLA	L-C-FA2
3	0.70	0.48	1.39	0.91	1.10
6	1.00	0.73	1.84	1.15	1.37
9	1.87	0.95	2.01	1.24	1.74
12	2.50	1.01	2.29	1.54	1.92

Table 6

Average carbonation depth in mm for the mixes for a total exposure period of 12 months

Fig. 5

Carbonation rate  
( $\text{mm}/\text{yr}^{1/2}$ ) for  
various mortar mixes  
exposed to coastal  
environment.



posites (Hsu et al., 2019) to maintain their workability (Table 4), while the partial substitution of cement by fine-grained additives simultaneously reduces the cement content in the mortars resulting the delay of the hydration process. According to the published materials, there exist few literatures that report the effect of fly ash addition on carbonation process (Qin et al., 2019), (Chen et al., 2021), (Czarnecki et al., 2018); these articles conclude that due to replacement of cement with fly ash, the rate of carbonation increases significantly. At the same time, the incorporation of fly ash leads to increased permeability of the hardened cement mortars at early ages; the latter effects on the resistance of mortar against carbonation and the diffusivity of  $\text{CO}_2$ . In our study, the three months carbonation depth increased by 2.0 and 1.6 times for L-F-FA1 and L-C-FA2 groups compared to Control group, while the specimens containing iron mill scale (SLA) were also 1.3 times more carbonated than OPC mortars. After 9 months of exposure in coastal environment it is also observed in the fly ash mixtures, that their carbonation coefficients are approximately equal to those of OPC mortars, while slag addition (SLA) reduced the carbonation by 33.7% at the same age; the latter is possibly the result of the formation of carbonate salts (ankerite, siderite) into the pores of mortars (Chousidis et al., 2016b). At the end of exposure (12 months), the additives used seems to further reduce the carbonation rates under than those of control mixture; the incorporation of pozzolanic materials such as fly ash leads to a reduction in porosity due to the chemical reaction of FA and  $\text{Ca}(\text{OH})_2$  (C-H) and the production of calcium silicate hydrate (C-S-H). Regarding the samples with E.M.D. waste addition, it can be observed that their carbonation depths have the lowest values among the mixtures tested for all ages. The carbonation reduction comparing with the mixture without additive, ranges from 31.4% to 59.5% for 3 and 12 months, respectively. It is generally recognized that the incorporation of fine materials such as E.M.D. leads to reduction in total and capillary porosity. Up to now, although some research results about the effect of E.M.D. waste on chloride penetration resistance have been published (Chousidis et al., 2015a), (Chousidis et al., 2020), the main attention of the aforementioned studies are related to the physic-mechanical properties of concrete. In this study, it is also proved the beneficial impact of E.M.D. additive on the carbonation resistance of cement mortars.

The average values (3 test samples) of porosity using MIP method for reinforced mortars placed in coastal environment are illustrated in Fig. 6. The cylinders were cured in a water tank for 7 days after casting and the tests were carried out at 6 and 12 months. From Fig. 6 a remarkable difference among the mixtures was detected; mortars containing FAs generally show higher porosity values

at 6 months than the other groups. On the other hand, E.M.D. and SLAG additions reduce the porosity of mortars compared to control mixture by 13.3% and 5.5% at the same age. At 12 months of exposure, it can be seen, that the composites and control mixtures appear lower values of porosity; this can be explained by the hydration of cement and C–S–H formation. The mortars blended with additives generally exhibit lower porosity values than those of the reference mortars at 12 months. This is attributed to the occurrence of amorphous phase in their chemical composition which participates to the pozzolanic reaction, while the fineness of additives also affects the salts formation into the pores of cementitious materials. In fact, fly ash contributes to the formation of Friedel's  $(Ca_4Al_2(OH)_{12}Cl_2 \cdot 4H_2O)$  and Kuzel's  $(Ca_4Al_2(OH)_{12}Cl(SO_4)_{0.5} \cdot 5H_2O)$  salts which may also lead to reduced porosity of concrete (Qiao et al., 2019), (Zhang et al., 2019), (Shaikh and Dobson, 2019). Concerning E.M.D. waste material is an ultrafine material filling the pores of concrete (Table 1), while it comprises hydrous sulfate salts  $(KFe^{3+}3(OH)_6(SO_4)_2)$  and thus affects its performance (Chousidis et al., 2020). It is worth mentioned that the porosity changes between 6 – 12 months is more obvious in the case of mortars containing FAs and ranges from 38.0% to 43.0%, while in respect of the other additives the change was 5.4% and 15.3% for E.M.D. and SLA, respectively.

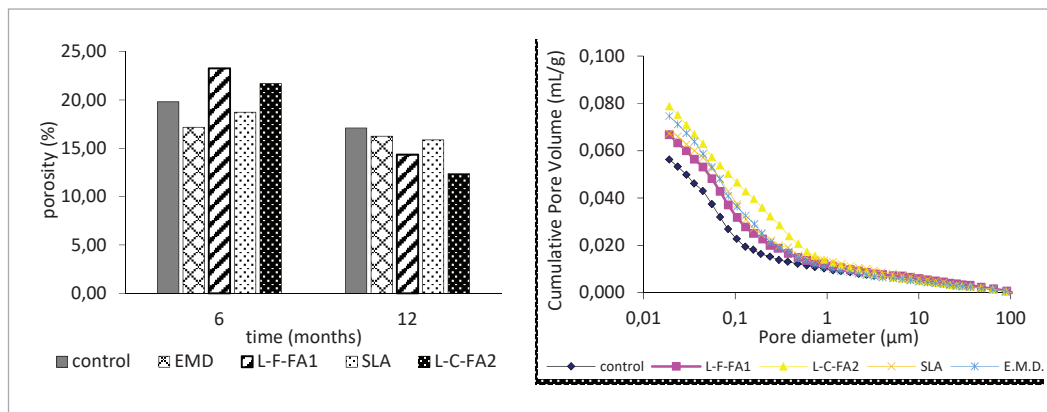


Fig. 6

Porosity (%) (left) and cumulative pore volume (mL/g) (right) for cement mortars after exposure in coastal environment

Fig. 7 represents the chloride content of mortars with and without additives calculated by Eq. 9 after exposure to coastal environment. The corrosion of the steel bars is triggered by the propagation of the chlorides through the pore solution to the reinforcement surface. The  $Cl^-$  ions can be either bound by the hydration products or they can exist as free ions in the pore solution. In our study we estimated the chloride concentration by  $AgNO_3$  titration method, which is fast, easy to perform and gives similar measured results among the methods used (He et al., 2012).

From Fig. 7, it is observed that the chloride contents increase when the exposure time increases for all mixes. The measurements show that the mixtures containing fly ash (L-F-FA1 & L-C-FA2), indicate higher chloride concentration compared to the other three (3) groups. It is known that the addition of supplementary cementitious materials (SCMs) with high reactive  $Al_2O_3$  and  $SiO_2$  contents, enhance the chloride binding, (Qiao et al., 2018), due to their chemical reaction with  $C_3A$ , forming calcium chloro-aluminate salt (Taylor, 1997). Except the above, chloride ions can be physically bound onto the surface of porous C–S–H particles due to their large surface area (Fu et al., 2020); this may be attributed by the ionic exchange between  $Cl^-$  ions and  $(OH)^-$  groups from the C–S–H layers (Hu et al., 2018) (Elakneswaran et al., 2009). On the other hand, mortars with iron mill scale (SLA) and E.M.D. waste exhibits low  $Cl^-$  amounts; the aforementioned additives have minor contents in aluminum, whilst the composites were also prepared with low amounts of cement due to its partial substitute by additives; so, the decreased  $C_3A$  in composite mortars leads to low chloride binding capacity. It can be also noted that the depassivation of steel rebars occurs

Fig. 7

Concentrations of chlorides in mortars after exposure to coastal conditions

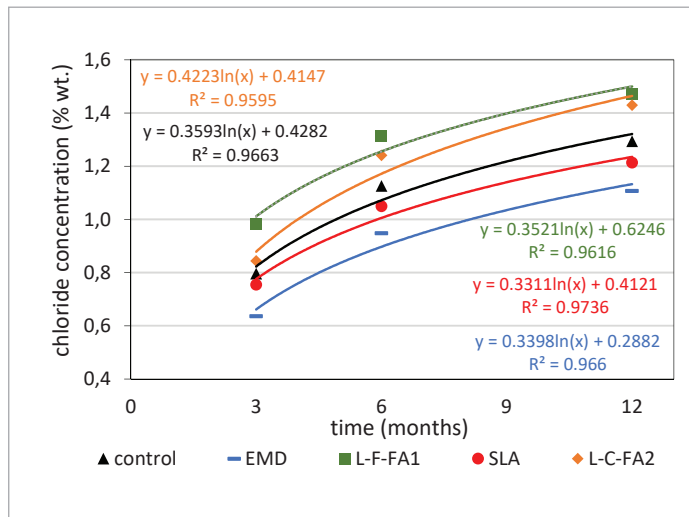
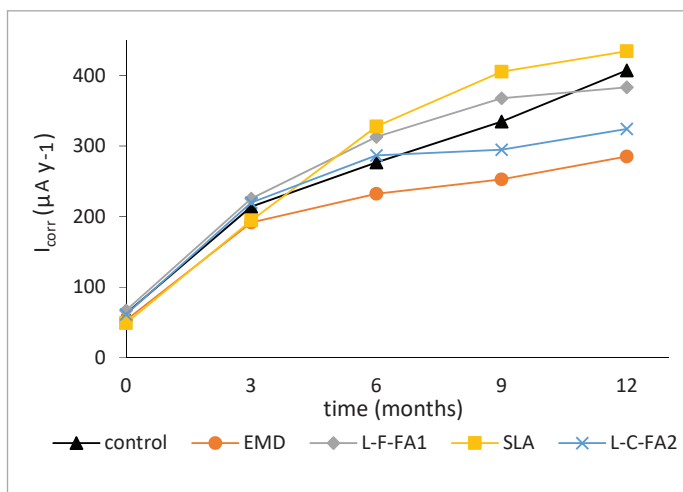


Fig. 8

Corrosion current densities ( $\mu\text{A y}^{-1}$ ) of the steel bars after 12 months of exposure in coastal environment



when the chloride content reaches a specific threshold value at the surface of the metal known as critical chloride threshold ( $C_{crit}$ ) (Cao et al., 2019), (Fakhri et al., 2021); however, only free-bound chlorides dispersed in the pore solution lead to the corrosion of the steel (Shi et al., 2012).

The corrosion current densities versus time for steel bars embedded in cement mortars are shown in Fig. 8. It can be seen that the reinforcement steel maintains its passivity for 10 – 15 days from the beginning of the measurements. Control and FA mortars seem to preserve the similar behavior up to three (3) months of exposure in corrosive environment. In contrast, at the same age, E.M.D. and SLA additives provide better anticorrosive protection in coastal environment; it has been previously proved, that iron mill scale (SLA) fills the

pores of mortar creating carbonate salts, while E.M.D. waste also reacts with the cement paste as an ultrafine material. Subsequently,  $I_{corr}$  clearly tends to be higher on L-F-FA1 and SLAG reinforced mortars (6 & 9 months), while L-C-FA2 specimens at 6 months showed almost equal  $I_{corr}$  values with the samples without additive. At the end of the measurements (12<sup>th</sup> month) only the mortars containing iron slag (SLA) exhibit higher  $I_{corr}$  values than OPC mortars by 6.7%; concerning the other 3 groups, E.M.D., L-C-FA2 and L-F-FA1 gave 30.0%, 20.4% and 5.8% lower  $I_{corr}$  values comparing with the reference mortar (control). It is worth noting that the metal remains in active state up to 12 months of exposure in coastal environmental conditions; however, steel rebars inserted in SLA, control and L-F-FA1 specimens demonstrate moderate to high corrosion ( $I_{corr} > 0.5 \mu\text{A}/\text{cm}^2$ ), while E.M.D. and L-C-FA2 low to moderate  $I_{corr}$  values ( $< 0.5 \mu\text{A}/\text{cm}^2$ ) (Andrade et al., 1990).

In the literature review, several studies have confirmed the beneficial effect of FA addition on the corrosion of reinforcing steel (Ha et al., 2007), (Boža and Topçu, 2012); this can be explained by the pozzolanic reaction between fly ash and hydrated cement paste resulting a denser microstructure over a period of time. However, the critical chloride threshold for the maintenance of its passivity is uncertain, because it depends on many factors such as the chemistry of FA, the amount of FA addition, the w/c ratio, the bound/free chlorides etc. Previous studies (Moghaddam et al., 2019), (Chousidis et al., 2016a) have revealed that the chloride penetration resistance of concrete increases with increasing the fineness of fly ash, while in medium to high (15 – 30%) FA additions also improve

the mechanical strength (Shi and Day, 1999) and the resistance to chloride and CO<sub>2</sub> deterioration mechanisms as well (Güneyisi et al., 2005), (Holland et al., 2016). Nevertheless, fly ash does not reduce the diffusion of chlorides at early ages, but at the later ages, significantly drops the diffusion coefficient as compared to control concrete (Basheer et al., 2001). In this study, the chemistry of additives and their fineness seem to play significant roles on the corrosion of steel reinforcement; considering the above parameters, FA additions provide the better anticorrosion protection on steel following by E.M.D. addition. On the other hand, the salts created into the pores of SLA mortars do not react with the chloride ions resulting the further corrosion of steel at late ages.

In order to evaluate the effectiveness of additives on chloride penetration resistance and corrosion of steel bars, mass loss measurements were conducted; the gravimetric mass loss and the cumulative mass loss for each steel bar were calculated from the difference between its initial and the final mass; the measurements are presented in Fig. 9 and 10. As depicted, the reinforcing steel embedded in mortars containing FA (L-C-FA2 and L-F-FA1) indicate slightly higher mass loss at early ages (3 & 6 months) due to the late pozzolanic reaction between fly ash and hydration products of cement. However, their small particle size and the glassy phase included into FA increase its pozzolanic reaction contributing to C-S-H formation at late ages; thus, fly ash addition led to decreased mass loss of the reinforcing steel at 12 months of exposure in saline environment.

Concerning SLA addition, it can be observed that the mass loss values were higher than those of mortar without any additive. As it described above, the pores of these composites fill with carbonate salts (ankerite and siderite) as a result of the reaction between Fe<sup>++</sup> and CO<sub>3</sub><sup>2-</sup> at late ages (>6 months); however, at the beginning of the measurements, the mortars blended with SLA indicate higher porosity than the conventional mixture resulting the entrance of chloride ions. It is worth noting that this material (SLA) is usually utilized as a replacement of sand for heavy-weight concrete production which used for radiation shielding or ballasting of pipes. Nevertheless, in this research, it was also proved its beneficial effect on the pitting corrosion of the reinforcing steel for the production cementitious mortars with a solid structure.

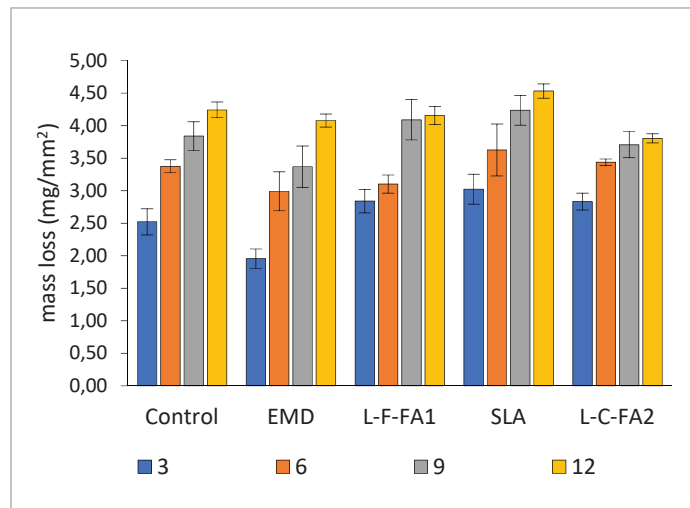


Fig. 9

Gravimetric mass loss (mg/mm<sup>2</sup>) of steel rebars exposed to coastal environment

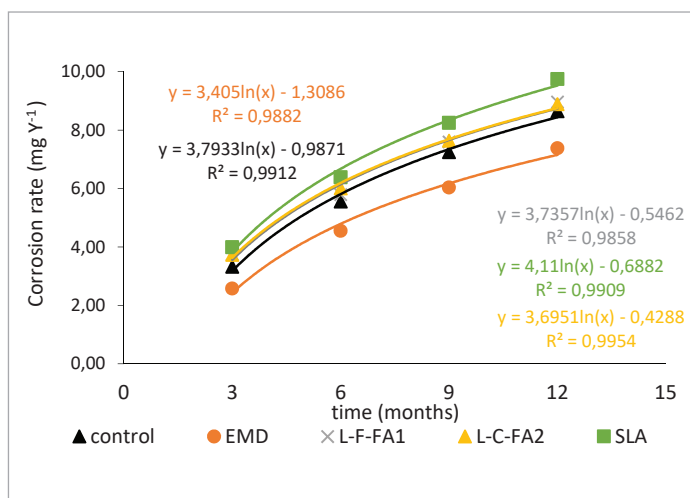


Fig. 10

Corrosion rate (mg Y<sup>-1</sup>) of steel rebars exposed to coastal environment

Fig. 11

Corrosion rate ( $\mu\text{m y}^{-1}$ ) for steel bars embedded in mortars and exposed to accelerated corrosion (salt spray cabin)

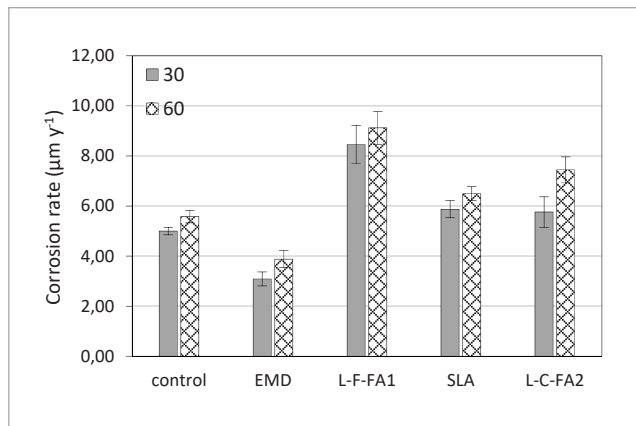
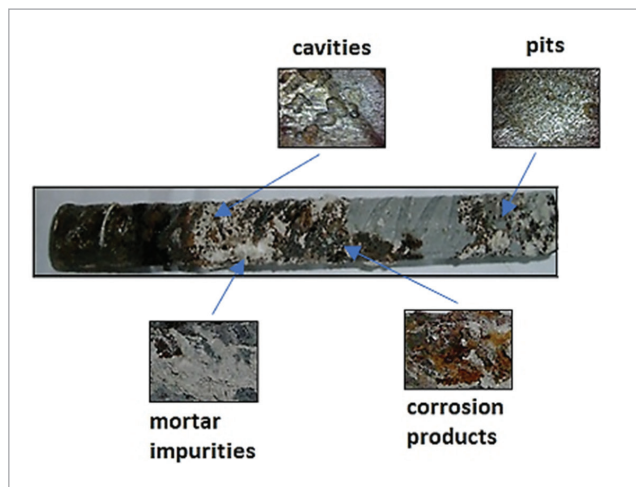


Fig. 12

Photograph of typical steel bar embedded in mortar after accelerated corrosion for 60 days



On the other hand, E.M.D. additive due to its fineness provides the better anticorrosion protection and corrosion rate values on steel re-bars up to 12 months of exposure in coastal environment. The aforementioned additive acts as a filler in the mortar mixture, thus further reducing the pore size of the hardened composite and generating more nucleation sites to accelerate hydration reactions.

The graph showing the corrosion rate (CR) of steel bars exposed in atmosphere and in salt spray cabin calculated are presented in Fig. 10 & 11, while Fig. 12 illustrates a corroded steel bar after accelerated corrosion. As can be seen, a progressive increase in steel corrosion is observed with increase of time for all examined groups. From Fig. 10 & 11, the composites have higher values of corrosion rate than those of conventional mortars; the latter is attributed to the replacement of cement by additives affecting on hydration process. It can be also observed that the E.M.D. decreased

the CR by 38.2% and 30.5% at 30 and 60 days compared to control group (Fig. 11); the equal decrease for the aforementioned group in coastal environment was 22% and 17.1% at 6 and 12 months, respectively. The improvement in corrosion of mortars with E.M.D. is due to the filling of the pores by the additive and thereby maintaining the perfect alkalinity near the steel anode.

## Conclusions

The following conclusions can be drawn from the present investigations:

- E.M.D. waste addition led to decreased mass loss, corrosion rate and  $I_{\text{corr}}$  of reinforcing steel at all measured ages. its high fineness compared to that of cement reduced the permeability of mortar.
- Fly ash up to the 10% replacement level improves the corrosion resistance properties of steel in concrete at 12 months of exposure in coastal environment. This is attributed to the fact that the FA additive has a pozzolanic activity, affecting cement hydration products ( $\text{C}_3\text{A}$ ,  $\text{C}_3\text{S}$ ,  $\text{C}_2\text{S}$ ), due to the presence of alumina ( $\text{Al}_2\text{O}_3$ ) and glass phase ( $\text{SiO}_2$ ) in its chemical composition.
- Iron mill scale led to decreased porosity values of mortar and may provide anticorrosion protection at early ages due to carbonate salts formation into the pores.
- Fly ash and iron mill scale mortars exhibited high carbonation rate after 6 months of exposure in coastal environment; at the same time, the carbonation values were lower in E.M.D. mortars comparing with the other groups.

## Conflict of Interest

The authors declare no financial or commercial conflict of interest.

- ANDRADE, C., ALONSO, M. C. & GONZALEZ, J. A. 1990. An Initial Effort to Use the Corrosion Rate Measurements for Estimating Rebar Durability. In: BERKE, N. S., CHAKER, V. & WHITING, D. (eds.). West Conshohocken, PA: ASTM International.
- BASHEER, L., KROPP, J. & CLELAND, D. J. 2001. Assessment of the durability of concrete from its permeation properties: a review. *Construction and Building Materials*, 15, 93-103. [https://doi.org/10.1016/S0950-0618\(00\)00058-1](https://doi.org/10.1016/S0950-0618(00)00058-1)
- BHAGATH SINGH, G. V. P. & SUBRAMANIAM, K. V. L. 2017. Direct decomposition X-ray diffraction method for amorphous phase quantification and glassy phase determination in binary blends of siliceous fly ash and hydrated cement. *Journal of Sustainable Cement-Based Materials*, 6, 111-125. <https://doi.org/10.1080/21650373.2016.1177478>
- BOĞA, A. R. & TOPÇU, İ. B. 2012. Influence of fly ash on corrosion resistance and chloride ion permeability of concrete. *Construction and Building Materials*, 31, 258-264. <https://doi.org/10.1016/j.conbuildmat.2011.12.106>
- CAO, Y., GEHLEN, C., ANGST, U., WANG, L., WANG, Z. & YAO, Y. 2019. Critical chloride content in reinforced concrete - An updated review considering Chinese experience. *Cement and Concrete Research*, 117, 58-68. <https://doi.org/10.1016/j.cemconres.2018.11.020>
- CHEN, T., BAI, M. & GAO, X. 2021. Carbonation curing of cement mortars incorporating carbonated fly ash for performance improvement and CO<sub>2</sub> sequestration. *Journal of CO<sub>2</sub> Utilization*, 51, 101633. <https://doi.org/10.1016/j.jcou.2021.101633>
- CHEN, W., HUANG, B., YUAN, Y. & DENG, M. 2020. Deterioration Process of Concrete Exposed to Internal Sulfate Attack. *Materials*, 13, 1336. <https://doi.org/10.3390/ma13061336>
- CHOUDHARY, R., GUPTA, R., ALOMAYRI, T., JAIN, A. & NAGAR, R. Permeation, corrosion, and drying shrinkage assessment of self-compacting high strength concrete comprising waste marble slurry and fly ash, with silica fume. *Structures*, 2021. Elsevier, 971-985. <https://doi.org/10.1016/j.istruc.2021.05.008>
- CHOUSIDIS, N., IOANNOU, I. & BATIS, G. 2018. Utilization of Electrolytic Manganese Dioxide (E.M.D.) waste in concrete exposed to salt crystallization. *Construction and Building Materials*, 158, 708-718. <https://doi.org/10.1016/j.conbuildmat.2017.10.036>
- CHOUSIDIS, N., IOANNOU, I., RAKANTA, E., KOUTSODONTIS, C. & BATIS, G. 2016a. Effect of fly ash chemical composition on the reinforcement corrosion, thermal diffusion and strength of blended cement concretes. *Construction and Building Materials*, 126, 86-97. <https://doi.org/10.1016/j.conbuildmat.2016.09.024>
- CHOUSIDIS, N., RAKANTA, E., IOANNOU, I. & BATIS, G. 2015a. Anticorrosive Effect of Electrochemical Manganese Dioxide By-Products in Reinforced Concrete. *Journal of Materials Science and Chemical Engineering*, Vol.03No.05, 12. <https://doi.org/10.4236/msce.2015.35002>
- CHOUSIDIS, N., RAKANTA, E., IOANNOU, I. & BATIS, G. 2015b. Mechanical properties and durability performance of reinforced concrete containing fly ash. *Construction and Building Materials*, 101, Part 1, 810-817. <https://doi.org/10.1016/j.conbuildmat.2015.10.127>
- CHOUSIDIS, N., RAKANTA, E., IOANNOU, I. & BATIS, G. 2016b. Influence of iron mill scale additive on the physico-mechanical properties and chloride penetration resistance of concrete. *Advances in Cement Research*, 28, 389-402. <https://doi.org/10.1680/jadcr.15.00129>
- CHOUSIDIS, N., ZACHAROPOULOU, A. K. & BATIS, G. 2020. Corrosion protection of reinforcement steel using solid waste materials in concrete production. *Magazine of Concrete Research*, 72, 271-277. <https://doi.org/10.1680/jmacr.17.00537>
- CZARNECKI, L., WOYCIECHOWSKI, P. & ADAMCZEWSKI, G. 2018. Risk of concrete carbonation with mineral industrial by-products. *KSCE Journal of Civil Engineering*, 22, 755-764. <https://doi.org/10.1007/s12205-017-1623-5>
- RILEM, R. 1988. CPC-18 Measurement of hardened concrete carbonation depth.
- ELAKNESWARAN, Y., NAWA, T. & KURUMISAWA, K. 2009. Electrokinetic potential of hydrated cement in relation to adsorption of chlorides. *Cement and Concrete Research*, 39, 340-344. <https://doi.org/10.1016/j.cemconres.2009.01.006>
- FAKHRI, H., FISHMAN, K. L. & RANADE, R. 2021. Rapid determination of critical chloride content in cement-based composites. *Construction and Building Materials*, 268, 121148. <https://doi.org/10.1016/j.conbuildmat.2020.121148>
- FU, C., YE, H., ZHU, K., FANG, D. & ZHOU, J. 2020. Alkali cation effects on chloride binding of alkali-activated fly ash and metakaolin geopolymers. *Cement and Concrete Composites*, 114, 103721. <https://doi.org/10.1016/j.cemconcomp.2020.103721>
- GÜNEYISI, E., ÖZTURAN, T. & GESOĞLU, M. 2005. A study on reinforcement corrosion and related properties of plain and blended cement concretes under different curing conditions. *Cement and Concrete Composites*, 27, 449-461. <https://doi.org/10.1016/j.cemconcomp.2004.05.006>

## References

- HA, T.-H., MURALIDHARAN, S., BAE, J.-H., HA, Y.-C., LEE, H.-G., PARK, K.-W. & KIM, D.-K. 2007. Accelerated short-term techniques to evaluate the corrosion performance of steel in fly ash blended concrete. *Building and Environment*, 42, 78-85. <https://doi.org/10.1016/j.buildenv.2005.08.019>
- HE, F., SHI, C., YUAN, Q., CHEN, C. & ZHENG, K. 2012. AgNO<sub>3</sub>-based colorimetric methods for measurement of chloride penetration in concrete. *Construction and Building Materials*, 26, 1-8. <https://doi.org/10.1016/j.conbuildmat.2011.06.003>
- HOLLAND, R. B., KURTIS, K. E. & KAHN, L. F. 2016. Effect of different concrete materials on the corrosion of the embedded reinforcing steel. In: POURSAEE, A. (ed.) *Corrosion of Steel in Concrete Structures*. Oxford: Woodhead Publishing. <https://doi.org/10.1016/B978-1-78242-381-2.00007-9>
- HSU, S., CHI, M. & HUANG, R. 2019. Influence of fly ash fineness and high replacement ratios on concrete properties. *Journal of Marine Science and Technology*, 27, 9.
- HU, X., SHI, C., YUAN, Q., ZHANG, J. & DE SCHUTTER, G. 2018. Influences of chloride immersion on zeta potential and chloride concentration index of cement-based materials. *Cement and Concrete Research*, 106, 49-56. <https://doi.org/10.1016/j.cemconres.2018.01.015>
- INTERNATIONAL STANDARD ORGANISATION 2009. ISO/DIS 8407.3, Corrosion of metals and alloys-Removal of corrosion products from corrosion test specimens. Genève, Switzerland.
- JOSHAGHANI, A., MOEINI, M. A., BALAPOUR, M. & MOAZENIAN, A. 2018. Effects of supplementary cementitious materials on mechanical and durability properties of high-performance non-shrinking grout (HPNSG). *Journal of Sustainable Cement-Based Materials*, 7, 38-56. <https://doi.org/10.1080/21650373.2017.1372318>
- KRISHNAMOORTHY, A. & KUMAR, G. M. 2013. Properties of green concrete mix by concurrent use of fly ash and quarry dust. *J. Eng.*, 3, 48-54. <https://doi.org/10.9790/3021-03834854>
- MEHTA, P. K. & GJØRV, O. E. 1982. Properties of portland cement concrete containing fly ash and condensed silica-fume. *Cement and Concrete Research*, 12, 587-595. [https://doi.org/10.1016/0008-8846\(82\)90019-9](https://doi.org/10.1016/0008-8846(82)90019-9)
- MENADI, B., KENAI, S., KHATIB, J. & AÏT-MOKHTAR, A. 2009. Strength and durability of concrete incorporating crushed limestone sand. *Construction and Building Materials*, 23, 625-633. <https://doi.org/10.1016/j.conbuildmat.2008.02.005>
- MOGHADDAM, F., SIRIVIVATNANON, V. & VES-SALAS, K. 2019. The effect of fly ash fineness on heat of hydration, microstructure, flow and compressive strength of blended cement pastes. *Case Studies in Construction Materials*, 10, e00218. <https://doi.org/10.1016/j.cscm.2019.e00218>
- PANDA, J. P., SANJAY, K., GHOSH, M. K. & SUB-BAIAH, T. Electrolytic Manganese Dioxide (EMD) From Manganese Cake-A Byproduct of Nodule Process. Eighth ISOPE Ocean Mining Symposium, 2009. ISOPE-M-09-017.
- QIAN, J., SHI, C. & WANG, Z. 2001. Activation of blended cements containing fly ash. *Cement and Concrete Research*, 31, 1121-1127. [https://doi.org/10.1016/S0008-8846\(01\)00526-9](https://doi.org/10.1016/S0008-8846(01)00526-9)
- QIAO, C., NI, W., WANG, Q. & WEISS, J. 2018. Chloride Diffusion and Wicking in Concrete Exposed to NaCl and MgCl<sub>2</sub> Solutions. *Journal of Materials in Civil Engineering*, 30, 04018015. [https://doi.org/10.1061/\(ASCE\)MT.1943-5533.0002192](https://doi.org/10.1061/(ASCE)MT.1943-5533.0002192)
- QIAO, C., SURANENI, P., NATHALENE WEI YING, T., CHOUDHARY, A. & WEISS, J. 2019. Chloride binding of cement pastes with fly ash exposed to CaCl<sub>2</sub> solutions at 5 and 23 °C. *Cement and Concrete Composites*, 97, 43-53. <https://doi.org/10.1016/j.cemconcomp.2018.12.011>
- QIN, L., GAO, X. & CHEN, T. 2019. Influence of mineral admixtures on carbonation curing of cement paste. *Construction and Building Materials*, 212, 653-662. <https://doi.org/10.1016/j.conbuildmat.2019.04.033>
- RAMEZANIANPOUR, A. A., RIAHI DEHKORDI, E. & RAMEZANIANPOUR, A. M. 2020. Influence of Sulfate Ions on Chloride Attack in Concrete Mortars Containing Silica Fume and Jajrood Trass. *Iranian Journal of Science and Technology, Transactions of Civil Engineering*, 44, 1135-1144. <https://doi.org/10.1007/s40996-020-00430-9>
- SCHLORHOLTZ, S. M. 1998. Soundness characteristics of portland cement-fly ash mixtures. *Cement, concrete and aggregates*, 20, 186-191. <https://doi.org/10.1520/CCA10453J>
- SELEEM, M., KHALIL, H. & ABU BAKR, M. 2020. Properties of Self-Compacting Concrete Incorporating Silica Fume and Fly Ash. (Dept. C). *MEJ. Mansoura Engineering Journal*, 38, 20-34. <https://doi.org/10.21608/bfemu.2020.107700>
- SHAIKH, F. U., NISHIWAKI, T. & KWON, S. 2018. Effect of fly ash on tensile properties of ultra-high performance fiber reinforced cementitious composites (UHP-FRCC). *Journal of Sustainable Cement-Based Materials*, 7, 357-371. <https://doi.org/10.1080/21650373.2018.1514672>
- SHAIKH, F. U. A. & DOBSON, J. 2019. Effect of fly ash on compressive strength and chloride binding of seawater-mixed mortars. *Journal of Sustainable Cement-Based Materials*, 8, 275-289. <https://doi.org/10.1080/21650373.2019.1582370>

- SHI, C. & DAY, R. L. 1999. Early strength development and hydration of alkali-activated blast furnace slag/fly ash blends. *Advances in Cement Research*, 11, 189-196. <https://doi.org/10.1680/adcr.1999.11.4.189>
- SHI, C. & STEGEMANN, J. A. 2000. Acid corrosion resistance of different cementing materials. *Cement and Concrete Research*, 30, 803-808. [https://doi.org/10.1016/S0008-8846\(00\)00234-9](https://doi.org/10.1016/S0008-8846(00)00234-9)
- SHI, X., XIE, N., FORTUNE, K. & GONG, J. 2012. Durability of steel reinforced concrete in chloride environments: An overview. *Construction and Building Materials*, 30, 125-138. <https://doi.org/10.1016/j.conbuildmat.2011.12.038>
- TAYLOR, H. F. 1997. *Cement chemistry*, Thomas Telford London. <https://doi.org/10.1680/cc.25929>
- VYRIDES, I., RAKANTA, E., ZAFEIROPOULOU, T. & BATIS, G. 2013. Efficiency of Amino Alcohols as Corrosion Inhibitors in Reinforced Concrete. *Open Journal of Civil Engineering*, Vol.03No.02, 8. <https://doi.org/10.4236/ojce.2013.32A001>
- WANG, X., WANG, K., LI, J., GARG, N. & SHAH, S. P. 2014. Properties of self-consolidating concrete containing high-volume supplementary cementitious materials and nano-limestone. *Journal of Sustainable Cement-Based Materials*, 3, 245-255. <https://doi.org/10.1080/21650373.2014.954155>
- WASHBURN, E. W. 1921. The Dynamics of Capillary Flow. *Physical Review*, 17, 273-283. <https://doi.org/10.1103/PhysRev.17.273>
- YODSUDJAI, W., VANRAK, P., SUWANVITAYA, P. & JUTASIRIWONG, A. 2020. Corrosion behavior of reinforcement in concrete with different compositions. *Journal of Sustainable Cement-Based Materials*, 1-20. <https://doi.org/10.1080/21650373.2020.1774440>
- ZAFEIROPOULOU, T., RAKANTA, E. & BATIS, G. 2013. Carbonation Resistance and Anticorrosive Properties of Organic Coatings for Concrete Structures. *JSEMAT*, VOL.3/1A, 67-74. <https://doi.org/10.4236/jsemat.2013.31A010>
- ZHANG, J., SHI, C. & ZHANG, Z. 2019. Chloride binding of alkali-activated slag/fly ash cements. *Construction and Building Materials*, 226, 21-31. <https://doi.org/10.1016/j.conbuildmat.2019.07.281>
- ZHANG, M., CHEN, J., LV, Y., WANG, D. & YE, J. 2013. Study on the expansion of concrete under attack of sulfate and sulfate-chloride ions. *Construction and Building Materials*, 39, 26-32. <https://doi.org/10.1016/j.conbuildmat.2012.05.003>
- ZHAO, J., WANG, D., WANG, X., LIAO, S. & LIN, H. 2015. Ultrafine grinding of fly ash with grinding aids: Impact on particle characteristics of ultrafine fly ash and properties of blended cement containing ultrafine fly ash. *Construction and Building Materials*, 78, 250-259. <https://doi.org/10.1016/j.conbuildmat.2015.01.025>

## NIKOLAOS CHOUSIDIS

### Postdoctoral Researcher

National Technical University of Athens,  
School Of Chemical Engineering, Department  
of Materials Science & Technology

### Main research area

Materials Engineering, Construction  
technology, nanotechnology, Corrosion  
Engineering, waste management

### Address

Iroon Polytechniou 9, Zografou 157 80,  
Athens, Greece  
Tel. 0030-6948802765  
E-mail: nickhous@central.ntua.gr

## GEORGE BATIS

### Professor Emeritus

National Technical University of Athens,  
School of Chemical Engineering, Department  
of Materials Science & Technology

### Main research area

Materials Engineering, Corrosion  
Engineering, corrosion inhibitors, waste  
management, Chemical Engineering

### Address

Iroon Polytechniou 9, Zografou 157 80,  
Athens, Greece  
Tel. 0030-2107723186  
E-mail: batis@chemeng.ntua.gr

## About the Authors

